

# INTERNATIONAL SOCIETY FOR SOIL MECHANICS AND GEOTECHNICAL ENGINEERING



*This paper was downloaded from the Online Library of the International Society for Soil Mechanics and Geotechnical Engineering (ISSMGE). The library is available here:*

<https://www.issmge.org/publications/online-library>

*This is an open-access database that archives thousands of papers published under the Auspices of the ISSMGE and maintained by the Innovation and Development Committee of ISSMGE.*

*The paper was published in the proceedings of the 10th European Conference on Numerical Methods in Geotechnical Engineering and was edited by Lidija Zdravkovic, Stavroula Kontoe, Aikaterini Tsiampousi and David Taborda. The conference was held from June 26<sup>th</sup> to June 28<sup>th</sup> 2023 at the Imperial College London, United Kingdom.*

*To see the complete list of papers in the proceedings visit the link below:*

<https://issmge.org/files/NUMGE2023-Preface.pdf>

# On the feasibility of data assimilation for uncertainty modelling in geotechnics

A. Amavasai<sup>1,2</sup>, T. Wood<sup>2</sup>, J. Dijkstra<sup>1</sup>

<sup>1</sup>*Chalmers University of Technology, Gothenburg, Sweden*

<sup>2</sup>*Ramboll Sweden AB*

**ABSTRACT:** Advanced constitutive models are usually employed in geotechnical applications to achieve higher fidelity solutions consequently demanding more model parameters. However, due to limited data availability, characterisation becomes difficult leading to increased uncertainties in the prediction which is quite common in geotechnical problems. In view of this, simpler models are preferred but sometimes are not robust enough to capture a complex geotechnical system. In this paper, we examine the issue of system uncertainty and model selection to gain a qualitative insight regarding the question of whether a simple model can capture a complex system when augmented with a data assimilation procedure, namely Ensemble Kalman Filter, while maintaining model fidelity and robustness. Results indicate that data assimilation can help capture the behaviour of the system even if the model complexity does not match that of the in-situ geotechnical system considered. The calibrated parameters can still capture the behaviour (be it simple or complex) beyond the assimilation window, however, for system with time dependent behaviour, longer monitoring time is required to enable simple models to reasonably capture the creep settlements demonstrating that a simple model would not always be sufficiently robust for modelling alternate scenarios that substantially change the complex system's behaviour.

**Keywords:** Data Assimilation, Ensemble Kalman Filter, system uncertainty, creep.

## 1 INTRODUCTION

Discrepancies exist between predicted and observed behaviour in geotechnical engineering since the forward models are only abstractions of the true state. Researchers resort to sophisticated techniques to improve the fidelity of the model making it more complex and challenging to use while general practitioners prefer simpler versions for better useability. So, the conflict between selecting an advanced or simple model relies not just on the system behaviour but also most importantly on the quality, accessibility and comprehensiveness of dataset of the observed behaviour to characterize corresponding model parameters. Given that a plethora of geotechnical models exist, practitioners still face the challenge to choose an appropriate model for which there is sparse information. This is a long-standing problem and is rarely studied in geotechnical engineering. Apart from limited data, the error in observed behaviour can also contribute to the difficulty in characterizing model parameters regardless of the model complexity used. As such, given the uncertainty of the model parameters, a deterministic assessment can further degrade the predictive ability of the considered model therefore demanding a probabilistic approach. Recent developments in other fields of science have shown a new powerful Bayesian updating procedure, known as

the Ensemble Kalman Filter (EnKF), a Data Assimilation (DA) technique, which systematically incorporates observations into numerical forecasting models accounting for the uncertainties from measurement and model parameters. The EnKF approximates the background error covariance matrix using a statistically consistent ensemble of states and as such they provide reasonable estimates of the state variables, i.e., deformation, pore pressure, or unknown parameters of the constitutive model in geotechnical practice as shown in recent works (Vardon et al., 2016; Liu et al., 2018; Tao et al., 2021). DA is a powerful tool holding great potential for geotechnical problems. When the geotechnical model is augmented with the EnKF algorithm, the uncertainties of the model parameters, characterized in a probabilistic manner, can be reduced when new project-specific monitoring data become available. However, the problem of model uncertainty still persists, and the performance of the numerical model combined with EnKF, even when it does not completely represent the geotechnical system is yet to be investigated. This study aims to provide some insight into whether it is possible for a geotechnical forward model, when augmented with a Data Assimilation procedure, to capture the geotechnical system behaviour that is not necessarily fully captured by the assumed numerical model (be it simple or advanced). Three constitutive models with differing, but hierarchical,

levels of complexity are considered in this study: Elastoplastic model, Elastoplastic model with structural degradation and an Elastoviscoplastic model with structural degradation. The general formulation for the EnKF and the aforementioned forward models are discussed in the coming sections. The insights gained from this study are expected to be useful to identify the effect of model uncertainty for application combining state and parameter estimation in geotechnical models.

## 2 THEORY

### 2.1 Principles of data assimilation

Given a monitoring window  $t \in [0, T]$  the evolution of the system state  $x_k \in R^m$  governed by the forward model  $F: f(t, x) \rightarrow f(t + \Delta t, x)$ ,  $V(t, x) \in [0, T] \times \Omega$ , is shown via the causality link in Equation (1). The true state of the system is measured through a set of observations modelled by  $y_k \in R^n$  in the observation space via the operator,  $H: f(t, x) \rightarrow g(t, x)$ ,  $V(t, x) \in [0, T] \times \Omega$  in Equation (2).

$$x_{k+1} = F(x_k) + q_k \quad (1)$$

$$y_k = H(x_k) + v_k \quad (2)$$

where the subscript 'k' denotes the timestep. The elements of the system state  $x_k$  comprise of displacement and porewater pressure at the nodes of the discretized system. ' $q_k$ ' is the process noise due to model error (which is implicitly taken into account from parameter uncertainty) and ' $v_k$ ' is the measurement noise. The error covariance matrix is then given as  $E[q_k q_k^T] \rightarrow Q_k$  and  $E[v_k v_k^T] \rightarrow R_k$ . By incorporating the latest observation likelihood  $p(x_k | y_{1:k-1})$  the posterior can be updated at time 'k' in Equation (3).

$$p(x_k | y_{1:k}) = \frac{p(y_k | x_k) p(x_k | y_{1:k-1})}{p(y_k | y_{1:k-1})} \quad (3)$$

The final goal of the data assimilation is to improve the state vector by obtaining the posterior distribution when monitoring data become available.

### 2.2 Ensemble Kalman Filter

The Ensemble Kalman Filter (EnKF) introduced by Evensen (2006) is based on the formulation of the Kalman Filter (Kalman, 1960) where the statistics of the state variable are represented by an ensemble of representations. This ensemble set is then forwarded in time by the nonlinear dynamics of the state evolution and analysed via the standard Kalman Filter analysis scheme to obtain the true posterior mean and variance at each time step. The ensemble representation of the forecast state vector is represented as

$$x_k^f = (x_k^{f,1}, x_k^{f,2}, x_k^{f,3}, \dots, x_k^{f,N}) \quad (4)$$

The mean, anomaly and the subsequent covariance matrix of the ensemble forecast state vector is given as

$$\hat{x}_k^f = \frac{1}{N} \sum_{n=1}^N x_k^{f,n} \quad (5)$$

$$X_k^f = \frac{1}{\sqrt{N-1}} (x_k^f - \hat{x}_k^f) \quad (6)$$

$$P_k^f = (X_k^f)(X_k^f)^T \quad (7)$$

An ensemble of perturbed observations with covariance matrix 'R' is defined.

$$y_k^j = y_k^t + v_k^j ; j = 1, 2, \dots, N \quad (8)$$

$$Y = \frac{1}{\sqrt{N-1}} [v_k^1, v_k^2, \dots, v_k^N] \quad (9)$$

$$R = Y Y^T \quad (10)$$

The Kalman gain 'K' is then obtained, and each ensemble member is updated in the analysis step

$$K = P_k^f H^T [H P_k^f H^T + R]^{-1} \quad (11)$$

$$x_k^{a,n} = x_k^{f,n} + K [y_{n,k} - H x_k^{f,n}] \quad (12)$$

where,  $n \sim (1, N)$

$$P_k^a = [I - K H] P_k^f \quad (13)$$

### 2.3 Geotechnical Forward models

In this study, an elastoviscoplastic constitutive model with structural degradation (denoted herein as **M3**) is implemented. The total strain rate is decomposed into elastic and viscoplastic strain components (Perzyna, 1966).

$$\dot{\varepsilon}_z = \dot{\varepsilon}_z^e + \dot{\varepsilon}_z^{vp} \quad (14)$$

The elastic part is denoted as

$$\dot{\varepsilon}_z^e = \kappa^* \frac{\dot{\sigma}_z'}{\sigma_z'} \quad (15)$$

where  $\kappa^*$  is the modified swelling index and  $\sigma_z'$  the vertical effective stress. The viscoplastic component based on Creep-SCLAY1S model (Gras et al., 2017) is proposed as

$$\varepsilon_z^{vp} = \frac{\mu_i^*}{\tau} \left\{ \frac{\sigma'_z (1 + \chi_0)}{[1 + \chi_0 \exp(-\rho \varepsilon_z^{vp})] \sigma'_{p0} \exp\left(\frac{\varepsilon_z^{vp}}{\lambda_i^* - \kappa^*}\right)} \right\}^{\frac{\lambda_i^* - \kappa^*}{\mu_i^*}} \quad (16)$$

For the elastic-plastic model (denoted herein as **M1**), the total strain rate consists of the elastic part (Equation (15)) and the elastic-plastic part. For stress levels beyond the apparent preconsolidation pressure,  $\sigma'_{p0}$ , the irrecoverable plastic strain is given as

$$\varepsilon_z^p = (\lambda^* - \kappa^*) \frac{\dot{\sigma}'_z}{\sigma'_z} \quad (17)$$

In this study, to account for destructuration effects in the elastoplastic model, the breakdown of the modified compression index to its intrinsic value is represented directly by proposing the relation below.

$$\varepsilon_z^p = \zeta \left[ 1 + \left( \frac{\psi}{\zeta} \right) \exp(-b \varepsilon_z^p) \right] \frac{\dot{\sigma}'_z}{\sigma'_z} \quad (18)$$

where  $\psi = (\lambda^* - \lambda_i^*)$ ,  $\zeta = (\lambda_i^* - \kappa^*)$  and 'b' is the scalar parameter defining the rate at which degradation occurs. This is different from the 'ρ' parameter used in M3 model to capture structural degradation. This model is denoted as **M2**. These 3 constitutive models with differing complexity are coupled with consolidation and discretized with the finite difference procedure (Rahman and Can Ulker, 2018; Yin and Graham, 1996) to solve the coupled partial differential equations for a one-dimensional settlement model simulated for an embankment loading. The parameters of all models are described in Table 1.

### 3 CASE STUDY

The problem geometry comprises of a single homogeneous soil layer of thickness, 'H' discretized using finite difference solution. An external load increment is applied at the top surface which is time dependent to simulate the construction of the embankment (3 m high and 20 m wide) until a specified time period. The embankment is built 3 m high with slope 1:2, on soil material of unit weight  $21 \text{ KN/m}^3$ . For simplicity, the true value of hydraulic conductivity is maintained to enable better comparison between different constitutive models. In this study, an error of 2 mm is chosen to generate noise from the true settlements. The synthetic noisy measurements for all 3 models are generated from simulations with known parameters as shown in Table 1. The prior knowledge of the uncertain parameters is assumed to follow a multivariate lognormal distribution from which 100 ensembles are generated for all cases.

Table 1. Description of parameters of all constitutive models along with the synthetic true values to generate observations

Parameters	Constitutive models		
	M1	M2	M3
Modified compressibility index, $\lambda^*$ (-)	0.27	0.27	-
Preconsolidation pressure, $\sigma'_p$ (kPa)	47	52	51
Modified swelling index, $\kappa^*$ (-)	0.025	0.025	0.025
Modified intrinsic compressibility index, $\lambda_i^*$ (-)	-	0.18	0.12
Destructuration constant, b (-)	-	10	-
Destructuration constant, ρ (-)	-	-	10.5
Structural parameter, $\chi_0$ (-)	-	-	7.5
Modified intrinsic creep index, $\mu_i^*$ (-)	-	-	2.7e-3
Reference time, τ (day)	-	-	1

#### 3.1 M1 model for capturing M2 soil behaviour

This section investigates whether M1 model in combination with the Ensemble Kalman Filter can be used to capture a soil behaviour where observations are synthetically generated with noise using M2 model with known parameters from Table 1. Table 2 shows the prior and final assimilated values of the M1 model parameters. The initial coefficient of variation (COV) is chosen as 0.15 for all parameters. Figure 1, 2 and 3 shows the back-calculated parameters of the M1 model with their corresponding confidence interval (1 standard deviation). It can be observed that the modified compressibility index ( $\lambda^*$ ) of M1 tries to reach a lower value mimicking the destructuration process of the M2 model. This shows that even when the feature of destructuration does not exist in M1, it can still be able to capture that feature if it exists in the system with the help of data assimilation. The low convergence rate of the modified swelling index ( $\kappa^*$ ) is attributed to its lower sensitivity (Tao et al., 2020). The preconsolidation pressure ( $\sigma'_p$ ), in this case, converges toward a smaller, but reasonably close, value than the ground truth. Figure 4 shows that M1 combined with EnKF provides an accurate forecast of the settlement against time than with just prior knowledge of the parameters. The calibrated parameters of M1 are subsequently used to predict the response beyond the time window used for DA, (i.e., beyond 2500 days). The settlement of the synthetic true system behaviour from the simulation is observed to be 0.6968 m while that from the calibrated parameters of the M1 model is around 0.6967 m at 5000 days making it a robust set of parameters. This shows that the calibrated parameters can capture the future behaviour beyond the monitoring window where no observations are available.

Table 2. List of prior knowledge of parameters and their post-assimilation values of Model M1

Parameters	Model M1			
	Prior		Final Assimilated	
	Mean	COV	Mean	COV
$\lambda^*$ (-)	0.245	0.15	0.203	0.02
$\sigma_p'$ (kPa)	55.5	0.15	50.3	0.01
$\kappa^*$ (-)	0.029	0.15	0.027	0.14

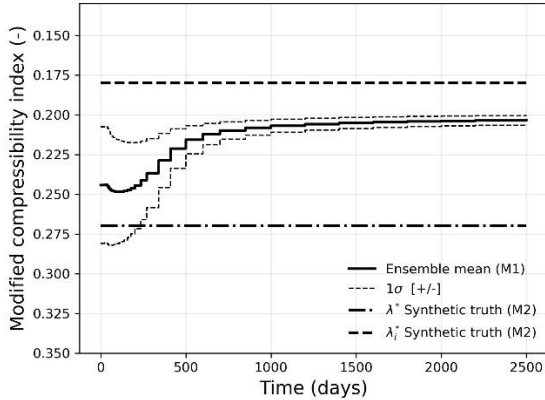


Figure 1. Convergence of modified compressibility index parameter from model M1

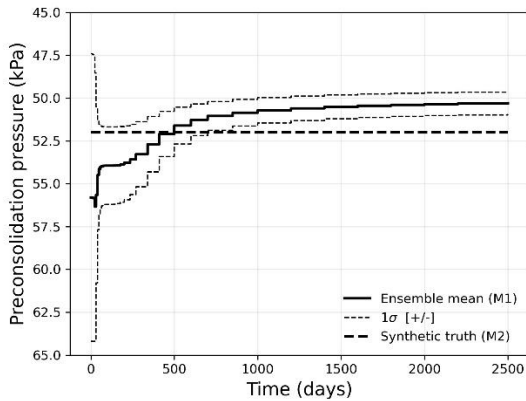


Figure 2. Convergence of preconsolidation pressure parameter from model M1

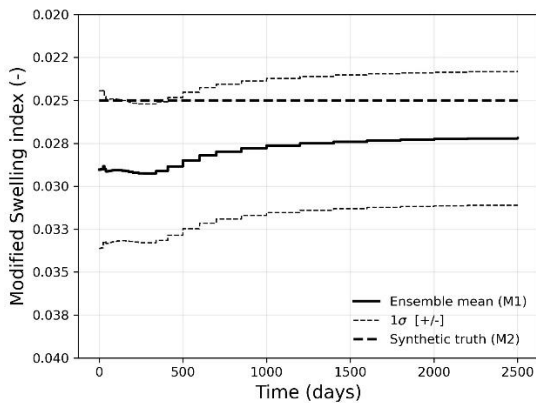


Figure 3. Convergence of modified swelling index parameter from model M1

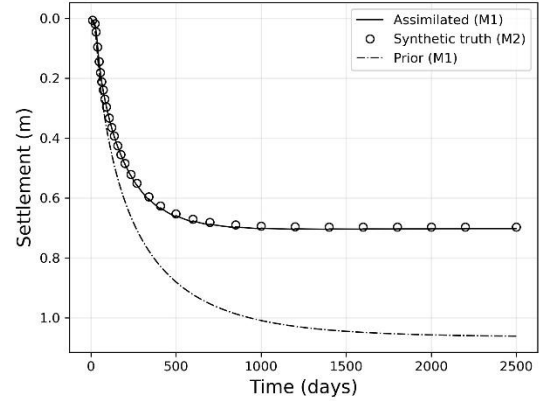


Figure 4. Comparison of settlement forecast between prior knowledge of parameters and using data assimilation

### 3.2 M2 model for capturing M1 soil behaviour

This section investigates whether a complex M2 model can capture a simpler system where observations are synthetically generated with noise using M1 with known parameters from Table 1. The convergence of the M2 parameters are not shown here for the sake of brevity but Table 3 shows the prior and final assimilated parameters along with their COV values for the M2 model. It can be observed that the destructuration parameter 'b' tends towards 0 and the modified intrinsic compressibility index ( $\lambda_i^*$ ) approaches a smaller value. This is expected as observed from the formulation of the M2 model in Equation (18) which now moves back to Equation (17) representing the M1 model. The preconsolidation pressure is captured reasonably accurately. The  $\lambda^*$  value is slightly elevated than the original true value since the 'b' parameter has not reached zero completely. The evolution of the gradient of the model M2 (see Figure 5) due to its structural degradation formulation attempts initially to reach the intrinsic value but as the observations get assimilated the gradient is pulled towards the M1 behaviour. The calibrated parameters of M2 are subsequently used to predict the response beyond the time window used for DA, (i.e., beyond 2500 days). The settlement from the true system behaviour is 0.9982 m while that from the assimilated parameters of the M2 model is around 0.9978 m at 5000 days making it a robust set of parameters.

Table 3. List of prior knowledge of parameters and their post-assimilation values of Model M2

Parameters	Model M2			
	Prior		Final Assimilated	
	Mean	COV	Mean	COV
$\lambda^*$ (-)	0.201	0.15	0.285	0.04
$\sigma_p'$ (kPa)	51.7	0.15	48.1	0.02
$\kappa^*$ (-)	0.029	0.15	0.023	0.13
$\lambda_i^*$ (-)	0.106	0.15	0.092	0.14
b (-)	7.5	0.15	0.81	0.12

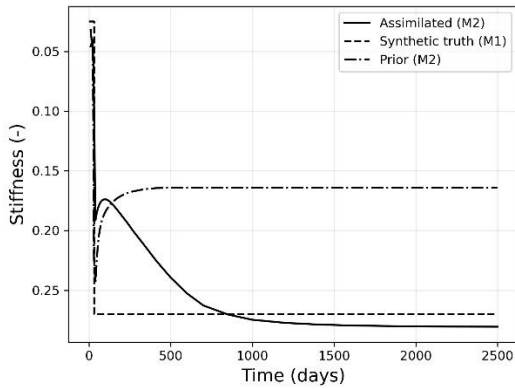


Figure 5. Convergence of stiffness toward M1 soil behaviour due to employed data assimilation

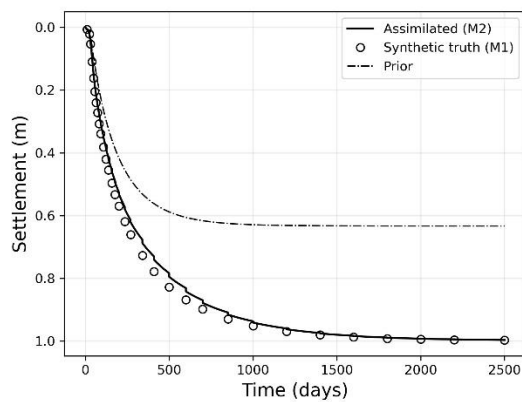


Figure 6. Comparison of settlement forecast between prior knowledge of parameters and using data assimilation

### 3.3 M1 and M2 model for capturing M3 soil behaviour

Although it is demonstrated that data assimilation can be a useful tool to capture the behaviour of the system with a model, not necessarily matching its complexity, it can be argued that both the M1 and M2 models are strictly hierarchical to each other which is believed to be the reason for the more or less compatible results. Furthermore, even beyond the monitoring window, the calibrated model parameters are still able to capture the future behaviour given incorrectly chosen model. However the latter finding need to be further investigated with a system which exhibits time dependent behaviour.

For the final case, a system with all the complex features from which observations are generated synthetically with noise using M3 model is considered (see Table 1 for parameters used to generate the synthetic data). The simpler models M1 and M2 are coupled with EnKF to investigate whether they can capture the M3 behaviour. As shown in Figure 7, the settlements are captured well using both models M1 and M2. In this case, in M1, the preconsolidation pressure goes to lower value far from the system truth with

elevated  $\lambda^*$  value. This is due to the compensation for the missing features from the M3 model. In contrast, for the M2 model, it is the intrinsic value  $\lambda_i^*$  that reaches a higher value since the ‘ $b$ ’ parameter is elevated due to the presence of structural degradation in the system. Similar to M1, M2 also shows convergence of  $\sigma_p'$  to lower values. Although most of the assimilated parameters goes beyond the physical meaning, it still show better performance from both these models in terms of settlement prediction in the short period. At 2500 days, the settlement of the true system is 1.2465 m. For M1, the prediction is 1.2515 m and M2 is 1.2479 m making M2 more accurate than the M1 model. In terms of precision both models achieve similar result when using data assimilation.

The calibrated parameters for models M1 and M2, are subsequently used to predict the response beyond the time window used for DA, i.e. beyond 2500 days (see Figure 8). Although a significant improvement from the prior knowledge can be observed, the results show that both models underpredict the future settlements when the calibrated parameters of M1 and M2 resulting from the DA procedure are used for future forecasts. This shows that the assimilated parameters are not robust in this case due to the presence of time-dependent deformations which both the models, the elastoplastic M1 and M2, fail to capture beyond the monitoring window. This deviation can be regarded as low for this particular static problem but for scenarios with large changes in the system’s boundary condition, the discrepancy can be severe. This finding underlines the importance of the fidelity of the forecasting model proving that a physically accurate model, of which the parameters and state variables are updated with DA, is always preferred that can be able to accurately predict the future state of the system.

Table 4. List of prior knowledge of parameters and their post-assimilation values of Model M1

Parameters	Model M1			
	Prior		Final Assimilated	
	Mean	COV	Mean	COV
$\lambda^*$ (-)	0.176	0.15	0.33	0.01
$\sigma_p'$ (kPa)	55.8	0.15	45.6	0.02
$\kappa^*$ (-)	0.029	0.15	0.018	0.14

Table 5. List of prior knowledge of parameters and their post-assimilation values of Model M2

Parameters	Model M2			
	Prior		Final Assimilated	
	Mean	COV	Mean	COV
$\lambda^*$ (-)	0.176	0.15	0.125	0.06
$\sigma_p'$ (kPa)	55.8	0.15	40.3	0.01
$\kappa^*$ (-)	0.029	0.15	0.022	0.13
$\lambda_i^*$ (-)	0.114	0.15	0.320	0.01
$b$ (-)	14.8	0.15	27.5	0.03

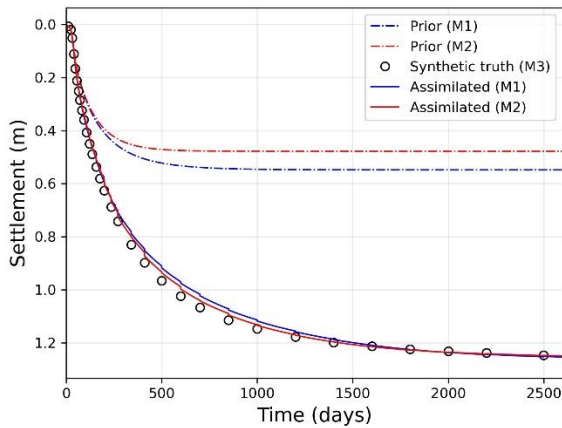


Figure 7. Comparison of settlement forecast of M1 and M2 models between prior knowledge of parameters and using data assimilation on a complex system.

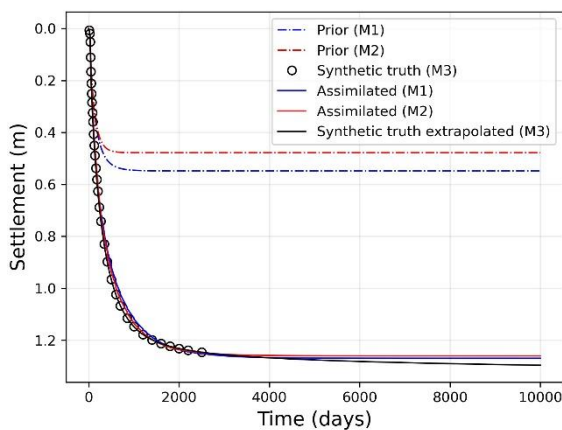


Figure 8. Investigation of long-term settlement prediction of both M1 and M2 models on a complex system

## 4 CONCLUSIONS

In this paper, the effectiveness of data assimilation in capturing the behaviour of the system even if the model complexity does not match that of the in-situ geotechnical system is studied. It is shown that by integrating the observations using Ensemble Kalman Filter, the model is able to capture the behaviour of the system (be it simple or complex) within the monitoring time window. Furthermore, using the calibrated parameters, the model is still able to capture the long term behaviour of the system well beyond the monitoring window where observations are not available. This shows that the choice of a suitable model is not based on capturing all the physical processes of the system as long as it is augmented with a data assimilation procedure. However, for system with time dependent behaviour, the calibrated parameters of the simpler non-viscous models struggle to capture the creep settlement beyond the monitoring window although the short term behaviour is well captured. Hence the assimilated parameters of the simpler models are not robust enough for scenarios that substantially

change the system's behaviour although a significant improvement is still achieved compared to the prior knowledge of the parameters. This can be partially alleviated by monitoring over longer duration which in most cases is not cost efficient. The findings in this study are based on a simplified numerical model to maintain computational efficiency but this can be scaled to more advanced numerical models to investigate the reliability of various geotechnical infrastructures involving different and complex stress paths.

## 5 ACKNOWLEDGEMENTS

The author would like to acknowledge the financial support from FORMAS under grant number 2020-00220.

## 6 REFERENCES

- Evensen, G. 2006. *Data Assimilation: The Ensemble Kalman Filter*, Springer, Berlin.
- Gras, J.-P., Sivasithamparan, N., Karstunen, M., Dijkstra, J. 2017. Strategy for consistent model parameter calibration for soft soils using multi-objective optimisation, *Computers and Geotechnics* **90**, 164–175.
- Kalman, R. E. 1960. A new approach to linear filtering and prediction problems, *Journal of Basic Engineering* **82**, 35–45.
- Liu, K., Vardon, P.J., Hicks, M.A. 2018. Sequential reduction of slope stability uncertainty based on temporal hydraulic measurements via the ensemble Kalman filter. *Computers and Geotechnics* **95**, 147–161.
- Perzyna, P. 1966. Fundamental problems in viscoplasticity, *Advances in Applied Mechanics* **9**, 243–377.
- Rahman, M., Can Ulker, M. 2018. *Modeling and Computing for Geotechnical Engineering, An Introduction*, CRC Press, Boca Raton.
- Tao, Y., Sun, H., Cai, Y. 2020. Predicting soil settlement with quantified uncertainties by using ensemble kalman filtering. *Engineering Geology* **276**, 101–115.
- Tao, Y., Sun, H., Cai, Y. 2021. Bayesian inference of spatially varying parameters in soil constitutive models by using deformation observation data. *International Journal for Numerical and Analytical Methods in Geomechanics* **45**, 1647–1663.
- Vardon, P.J., Liu, K., Hicks, M.A. 2016. Reduction of slope stability uncertainty based on hydraulic measurement via inverse analysis. *Georisk: Assessment and Management of Risk for Engineered Systems and Geohazards* **10**, 223–240.
- Yin, J. H., Graham, J. 1996. Elastic visco-plastic modelling of one-dimensional consolidation, *Géotechnique* **46**, 515–527.